

SUBJECT: SOI – Geophysical Assistance

December 10, 2009

TO: Craig R. Derickson
State Conservationist
NRCS, Harrisburg, Pennsylvania

File Code: 330-7

Dr. Henry Lin
Assistant Professor of Hydropedology/Soil Hydrology
Crop & Soil Sciences Department
415 Agricultural Sciences and Industries Building
Pennsylvania State University
University Park, PA 16802

Purpose:

At the request of the Dr. Henry Lin, Associate Professor of Hydropedology, geophysical field assistance was provided by the National Soil Survey Center to the Department of Crop and Soil Sciences at Pennsylvania State University. Geophysical investigations were conducted within the Shale Hills *Critical Zone Observatory (CZO)* in Huntington County, and at Pennsylvania State University's Klepler Farm in Centre County. Jim Doolittle also provided a lecture and field demonstration on the uses of geophysical techniques in soils and hydropedologic investigations to one of Dr. Lin's classes. The primary purpose of this assistance was to use GPR to study the infiltration of water in a small, steeply-sloping, forested catchment in which the soils are developing upon highly folded and fractured shale parent rock.

Participants:

Doug Baldwin, Graduate Student, Department of Crop & Soil Sciences, PSU, University Park, PA
Jim Doolittle, Research Soil Scientist, USDA-NRCS-NSSC, Newtown Square, PA
Chris Graham, PhD Student, Department of Crop & Soil Sciences, PSU, University Park, PA
Henry Lin, Assistant Professor of Hydropedology/Soil Hydrology, Department of Crop & Soil Sciences, PSU, University Park, PA
Jun Zhang, PhD Student, Department of Crop & Soil Sciences, PSU, University Park, PA

Activities:

Field activities were completed during the period of 11 and 12 November 2009.

Summary:

1. Detailed, repetitive ground-penetrating radar (GPR) surveys of an *infiltration grid site* were conducted with a 400 MHz antenna. The *infiltration grid site* (150 by 90 cm) is located in an area of Rushtown soils within the Shale Hills CZO. Twenty-four separate GPR surveys of this grid site were completed over a two day period. Each GPR survey consisted of 10 separate radar traverses and records (total of 264 radar records). During the first day, 20 liters of water were emptied into a shallow (about 15 cm deep) hole (diameter of about 10 cm), which was located in the upslope portion of the grid area. On day one, a constant head of water was maintained in this hole for eight radar surveys. To measure changes in soil moisture, twenty Decagon 5TE soil moisture sensors were inserted in a trench, which is located immediately down slope of the grid area.
2. Two, detailed GPR surveys were also completed across a *permanent grid site*, which is also located in another area of Rushtown soils.
3. Copies of the radar records that were collected over the two grid sites have been turned-over to the principal investigator, Jun Zhang, for analysis. As part of his research project, Jun is responsible for the

analysis of the collected two-dimensional (2D) radar records and the construction and interpretation of three-dimensional (3D) pseudo-images. Data collected during this two-day period are essential to Jun's research on the infiltration of water in shallow soils underlain by highly fractured shale.

4. A presentation was provided to Dr Lin's Hydropedology class on the afternoon of 11 November. Following this presentation, hands-on field demonstrations of both GPR and electromagnetic induction (EMI) was provided at PSU's Klepler Farm.
5. The synergy of GPR and global positioning systems (GPS) were explored at both Klepler Farm and in the Shale Hills Catchment area. Problems were encountered with satellite reception in the Shale Hills Catchment area. Subsequent visits with a Trimble field representative revealed that the GPS receiver was malfunctioning. It has been returned to Trimble for repairs. When problems are corrected, further evaluations of the use of these techniques are required. These studies should include the collection of ground-truth soil core data to verify GPR depth determinations.

/s/ Jonathan W. Hempel

JONATHAN W. HEMPEL
Director
National Soil Survey Center

cc: See attached list

cc:

Larry W. West, National Leader, Soil Survey Research & Laboratory, NSSC, MS 41, NRCS, Lincoln, NE

Edgar White, State Soil Scientist, NRCS, Harrisburg, PA

Jim Doolittle, Research Soil Scientist, NSSC, NRCS, Newtown Square, PA

Steve Carpenter, MLRA Office Leader, USDA-NRCS, Morgantown, WV

Michael Golden, Director of Soils Survey Division, USDA-NRCS, Washington, DC 20250

Wes Tuttle, Soil Scientist (Geophysical), USDA-NRCS-NSSC, Wilkesboro, NC 28697

L. West, National Leader for Soil Survey Research and Laboratory Staff, USDA-NRCS-NSSC, Lincoln, NE

Mike Wilson, Research Soil Scientist & Liaison for MO13, Soil Survey Research and Laboratory Staff, USDA-NRCS-NSSC, Lincoln, NE

Technical Report on Geophysical Investigations conducted at the Shale Hills *Critical Zone Observatory (CZO)* in Huntington County and at Pennsylvania State University's Klepler Farm in Centre County on 11 and 12 November 2009.

James A. Doolittle

Equipment:

The radar unit is the TerraSIRch Subsurface Interface Radar (SIR) System-3000 (SIR-3000), manufactured by Geophysical Survey Systems, Inc. (GSSI; Salem, NH).¹ The SIR-3000 consists of a digital control unit (DC-3000) with keypad, SVGA video screen, and connector panel. A 10.8-volt lithium-ion rechargeable battery powers the system. The SIR-3000 weighs about 9 lbs (4.1 kg) and is backpack portable. With an antenna, the SIR-3000 requires two people to operate. Daniels (2004) and Jol (2008) discuss the use and operation of GPR. The 200 and 400 MHz antennas were used in this investigation. Both a Trimble AgGPS 114 L-band DGPS (differential GPS) receiver and a Pathfinder ProXT GPS receiver with Hurricane antenna (Trimble, Sunnyvale, CA) were used to georeferenced GPR data.¹

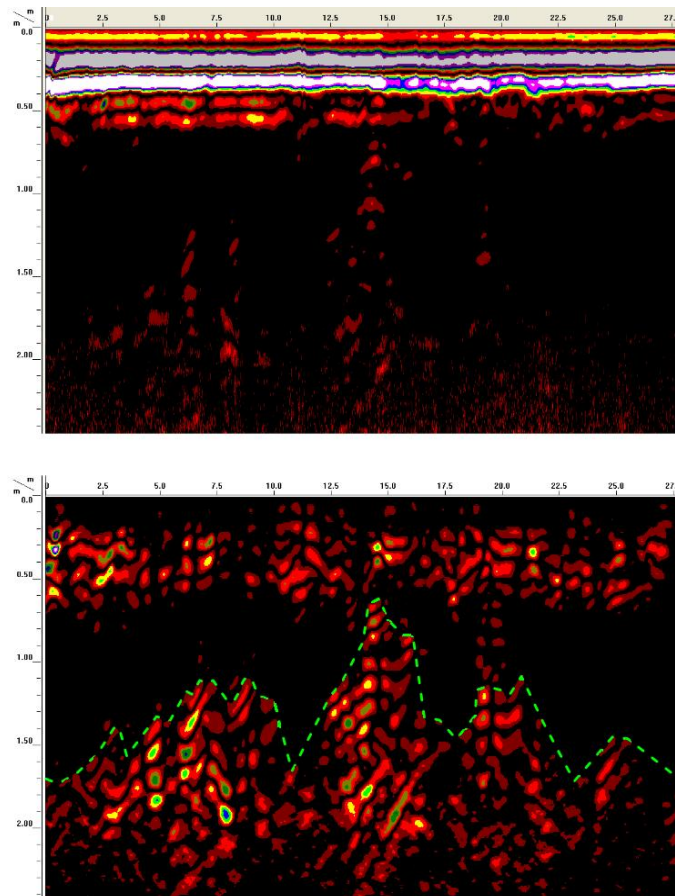


Figure 1. Unprocessed (upper) and processed (lower) images of the same radar record that was collected in an area of Hagerstown silt loam, 3 to 8 percent slopes (HaB). On the processed radar record, a green-colored dashed line has been used to identify the contact of the soil with the underlying limestone bedrock.

¹ Manufacturer's names are provided for specific information; use does not constitute endorsement.

The RADAN for Windows (version 6.6) software program (GSSI) was used to process the radar records.¹ Basic processing steps that were applied to all radar records include: header editing, setting the initial pulse to time zero, color table and transformation selection, display range gain adjustments. Migration, horizontal filtration, signal stacking, and range gain adjustment processing procedures were applied to improve the clarity and interpretability of subsurface interfaces appearing on radar records and imagery shown in this report. Figure 1 contains an unprocessed (upper record) and processed (lower record) image of the same radar record, which was collected in an area of Hagerstown silt loam, 3 to 8 percent slopes (HaB) at Klepler Farm in Centre County. Both radar records were subjected to the same basic processing procedures that are listed above. In addition, migration, horizontal filtration, signal stacking, and range gain adjustment processing procedures were applied to the lower radar record shown in Figure 1. On this (lower) radar record, a green-colored dashed line has been used to identify the interpreted depth to the underlying limestone bedrock. Though this interface is highly segmented with absent or weak reflections in many places, the soil-bedrock interface is, at least, interpretable on the more highly processed than on the relatively unprocessed radar record. This example provides proof, that, with the use of several advanced image processing techniques, the soil-bedrock interface can be interpreted with reasonable confidence in many areas of Hagerstown and Opequon soils.

Calibration of GPR:

Ground-penetrating radar is a time scaled system. The system measures the time that it takes electromagnetic energy to travel from an antenna to an interface (e.g., bedrock, soil horizon, stratigraphic layer) and back. To convert the travel time into a depth scale, either the velocity of pulse propagation or the depth to a reflector must be known. The relationships among depth (D), two-way pulse travel time (T), and velocity of propagation (v) are described in equation [1] (after Daniels, 2004):

$$v = 2D/T \quad [1]$$

The velocity of propagation is principally affected by the relative dielectric permittivity (E_r) of the profiled material(s) according to equation [2] (after Daniels, 2004):

$$E_r = (C/v)^2 \quad [2]$$

Where C is the velocity of propagation in a vacuum (0.298 m/ns). Typically, velocity is expressed in meters per nanosecond (ns). In soils, the amount and physical state (temperature dependent) of water have the greatest effect on the E_r and v. At the time of these studies, soils were relatively dry.

Based on the measured depth and the two-way pulse travel time to a known subsurface reflector (metal plate buried at 50 cm), the velocity of propagation and the relative dielectric permittivity through the upper part of soil profiles were estimated using equations [1] and [2]. In an area of Rushtown soils, the estimated E_r was 10.53. This permittivity resulted in a v of 0.0918 m/ns.

Field Methods:

The Shale Hills Catchment is underlain by fractured rock. In this study, GPR and frequency-domain reflectometry (FDR) are used to better understand and characterize ground-water flow paths in very deep soils over fractured bedrock, at scales of one to several meters. The infiltration grid site is located in a swale and in an area of Rushtown soils. The very deep, excessively drained Rushtown soils formed in colluvial deposits. Rushtown is a member of the loamy-skeletal over fragmental, mixed, active, mesic Typic Dystrudepts taxonomic family.

The dimensions of the infiltration grid are 150 by 90 cm. To complete a GPR survey, ten, 150-cm traverses are completed across the grid with a 400 MHz antenna. Traverse lines are orientated essentially orthogonal to the slope. The interval between successive traverse lines is 10 cm. Thirteen and twelve separate GPR surveys of the *infiltration grid site* were completed on days one and two, respectively. Each survey consisted of 10 parallel

GPR traverses, which were conducted from west to east across the grid site. Over this two-day period, about 20 liters of water were emptied into a shallow (about 15 cm deep) hole (about 10 cm in diameter) located within the grid and near the northeast corner. On day one, water was emptied into the hole and a constant head was maintained for 75 minutes. No water was emptied into the hole on the second day. Ground-penetrating radar surveys were completed at ten minute intervals on both days. Some water was observed seeping into the downslope trench along exposed root channels. At no time during this experiment did water flow across the surface of the *infiltration grid site*.

Twenty Decagon 5TE sensors (Pullman, Washington) were installed in the downslope trench.² These sensors were inserted into the upslope sidewall at depths of 5, 10 and 20 cm. These sensors are designed to measure soil moisture, soil temperature, and bulk electrical conductivity (EC).

Results:

GPR Survey of Infiltration Grid:

Repetitive GPR surveys were conducted across the small *infiltration grid site* to observe temporal differences in subsurface reflections associated with the flow of water through profiles of Rushtown soils. Appendix 1 lists the radar file numbers associated with different traverses both within and outside the infiltration grid site.

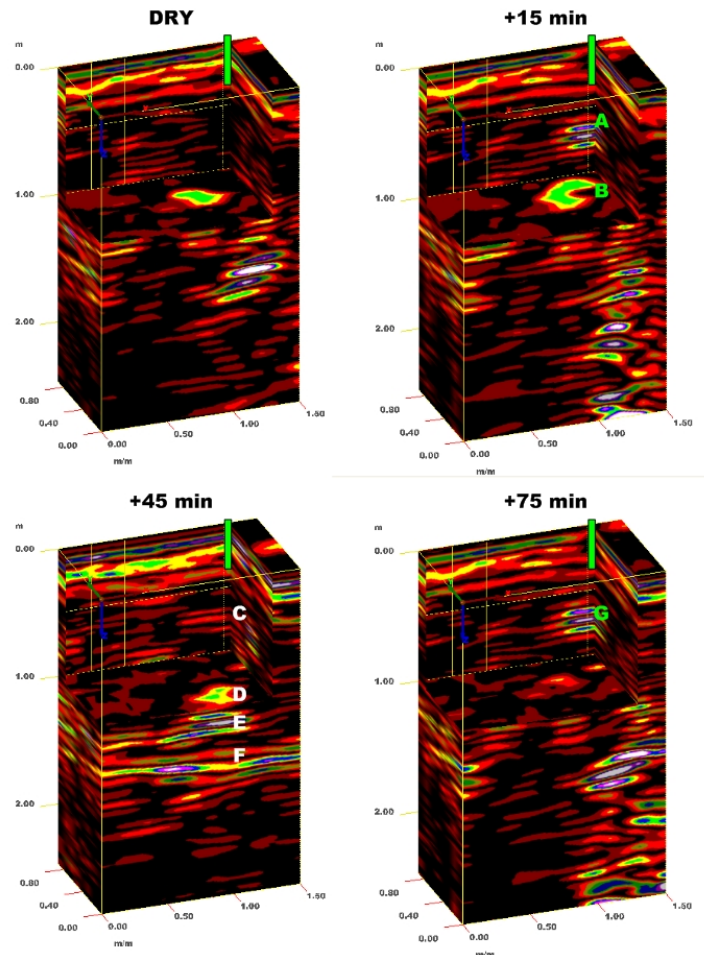


Figure 2. These 3D pseudo-images of the infiltration grid site were collected under the initial dry conditions (DRY), and 15, 45, and 75 minutes after achieving constant head in the infiltration hole. The infiltration hole is represented by the green-colored column in the upper portion of each 3D pseudo-image. All measurements are expressed in meters.

² Manufacturer's names are provided for specific information; use does not constitute endorsement.

Figure 2 contains four pseudo-images of the *infiltration grid site*. In these images, all measurements are expressed in meters. Radar records used to prepare these pseudo-images were from grid surveys that were conducted (1) prior to wetting, (2) 15 minutes after constant head, (3) 45 minutes after constant head, and (4) 75 minutes after constant head in the infiltration hole (all on day one). All radar records used to prepare these pseudo-images were subjected to the same processing procedures, which included: header editing, setting the initial pulse to time zero, color table and transformation selection, and distance normalization. After initial the processing, each set of radar records were combined into a 3D radar file, which was migrated and stacked. Migration was used to reduce noise associated with hyperbolic diffraction patterns and more properly align inclined interfaces. A 2D constant velocity migration was performed on all 3D radar files. All radar records shown in Figure 2 are displayed with the same display range gain adjustments.

In each of the radar records shown in Figure 2, inclined reflection patterns are evident. These reflectors vary in amplitude and expression, and are believed to represent different strata within the colluvium. Strata vary in grain-size distribution, rock fragments, moisture, and/or density. The higher the amplitude of the reflected signals (in Figure 2, high-amplitude reflections are colored white, blue, green, and yellow) the more abrupt and contrasting the difference in dielectric properties across the interface. Some variations in reflective patterns and amplitudes on these 3D pseudo-images are caused by variations in the placement of the radar traverse, and antenna alignment and jarring.

In Figure 2, the location of the infiltration hole has been approximated by a green-colored column at the top of each pseudo-image. Approximately 15 minutes after attainment of a constant head in the infiltration hole, a high-amplitude reflection has appeared near “A” (see upper-right pseudo-image in Figure 2). This reflection is believed to be caused by infiltrating water and represents a contact between drier and moister soil materials. In the same pseudo image (+ 15 minutes), a relatively high-amplitude subsurface spatial pattern (see “B”), appears to have enlarged and migrated down slope. Approximately 45 minutes after attainment of a constant head in the infiltration hole, the previously recognized high-amplitude reflection (see “A” in upper-right pseudo-image) appears to have weakened in amplitude immediately beneath the infiltration hole, but to have moved and extended down slope (see “C” in the lower-left pseudo-image in Figure 2). Once again, these patterns are believed to represent the migration of water through the soil. The subsurface pattern identified as “B” in the + 15 minute pseudo-image (upper-right image), after 45 minutes of constant head in the infiltration hole, continues to move down slope (see “D” in lower-left image). At this moment in time (plus 45 minutes), two subsurface interfaces (see “E” and “F”), which represent different layers of colluvium, become most highly expressed. Could this increased expression be the result of water moving along these formerly drier surfaces? Approximately 75 minutes after attainment of a constant head in the infiltration hole, a high-amplitude reflection reappears beneath the infiltration hole (see “G” in lower-right pseudo-image in Figure 2). No explanation for this high-amplitude reflector is possible at this time other than variations in antenna positioning. The two subsurface interfaces (“E” and “F”) identified in the plus 45 minute pseudo-image, are less well expressed in the plus 75 minutes pseudo-image. This can be explained by the expansion of the wetting front and the more gradational the change in moisture contents across these interfaces. At this moment in time, the suspected added moisture on either side of these interfaces appears to have reduced the electromagnetic gradient across these interfaces.

The same composite radar records and 3D pseudo-images that are shown in Figure 2 are shown again in Figure 3. In Figure 3, however, the data have been transformed using a Hilbert transformation envelope. Hilbert transformation uses the magnitude of the return signal to decompose multiple hyperbolic reflections into more compact and representative forms (Daniels 2004). What appears obvious on these transformed pseudo-images is the vertical extension of high magnitude signals after the infiltration experiment was begun (see Figure 3, +15 min and +45 min images), and later, the subsequent partial decay of these magnitudes as (supposedly) water permeated the subsurface, which became more uniformly wetted and less contrasting. If this interpretation is correct, these patterns suggest that moisture moves more rapidly downward than laterally through this area of Rushtown soils.

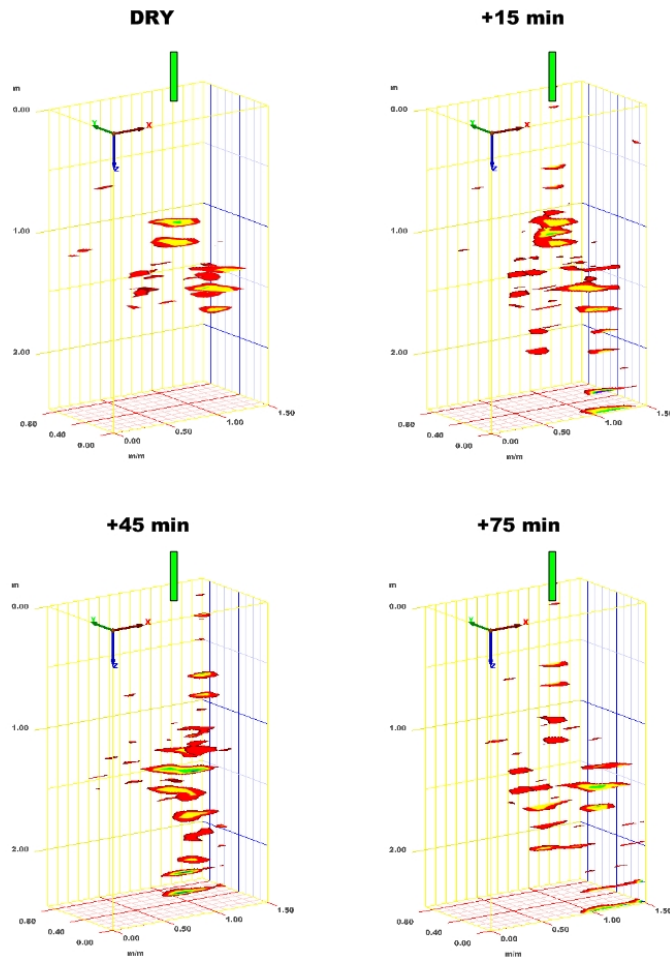


Figure 3. Data shown in these 3D pseudo-images have been transformed using a Hilbert transform envelope. These 3D pseudo-images of the infiltration grid site were collected under the initial dry conditions (DRY), and 15, 45, and 75 minutes after achieving constant head in the infiltration hole. The infiltration hole is represented by the green-colored column in the upper portion of each 3D pseudo-image. All measurements are expressed in meters.

GPR-GPS:

The SIR-3000 system provides a setup for the simultaneous use of a GPS receiver and serial data recorder (SDR). This setup georeferences GPR data for display in imaging software such as Google Earth and geographic information systems (GIS). With this setup, each scan on a radar record is essentially georeferenced (position/time matched). GPR readings (scans) are not continuous, but are taken at set time intervals. In this study, the scanning rate was 64 scans/sec. Position data were recorded at a rate of one measurement/sec with the Trimble ProXT GPS receiver. In RADAN, the position of each radar scan is proportionally adjusted according to the time stamp of the two nearest positions recorded with the GPS receiver. As each scan of the radar is georeferenced, the integration of GPS with GPR results in incredibly large data sets.

Using the *Interactive Interpretation* module of the RADAN for Windows software program, depths to the soil-bedrock interface were quickly, automatically, and reasonably accurately picked and outputted to a worksheet (X, Y, Z format; containing latitude, longitude, depths to contrasting interface, and other useful data). Using the *Interactive Interpretation* module, radar data can be easily exported into Microsoft Excel for documentation and analysis and GIS for plotting and visualization.

Klepler Farm:

A radar traverse was conducted along a research field boundary and across areas mapped as Hagerstown silt loam, 3 to 8 percent slopes (HaB); and Opequon-Hagerstown complex, 3 to 8 percent slopes (OhB). The well drained, deep and very deep Hagerstown and shallow Opequon soils formed in residuum weathered from limestone. Hagerstown and Opequon soils are members of the fine, mixed, semiactive, mesic Typic Hapludalfs; and clayey, mixed, active, mesic Lithic Hapludalfs taxonomic families, respectively. Because of their high clay contents and respective depths to bedrock, Hagerstown and Opequon soils are considered to have low and moderately potential for GPR), respectively (<http://soils.usda.gov/survey/geography/maps/GPR/index.html>). As discussed earlier in this report, following extensive processing, in areas of deep and very deep Hagerstown soils, the soil-bedrock interface was interpreted on radar records with reasonable confidence and to greater than anticipated depths (<100 cm).

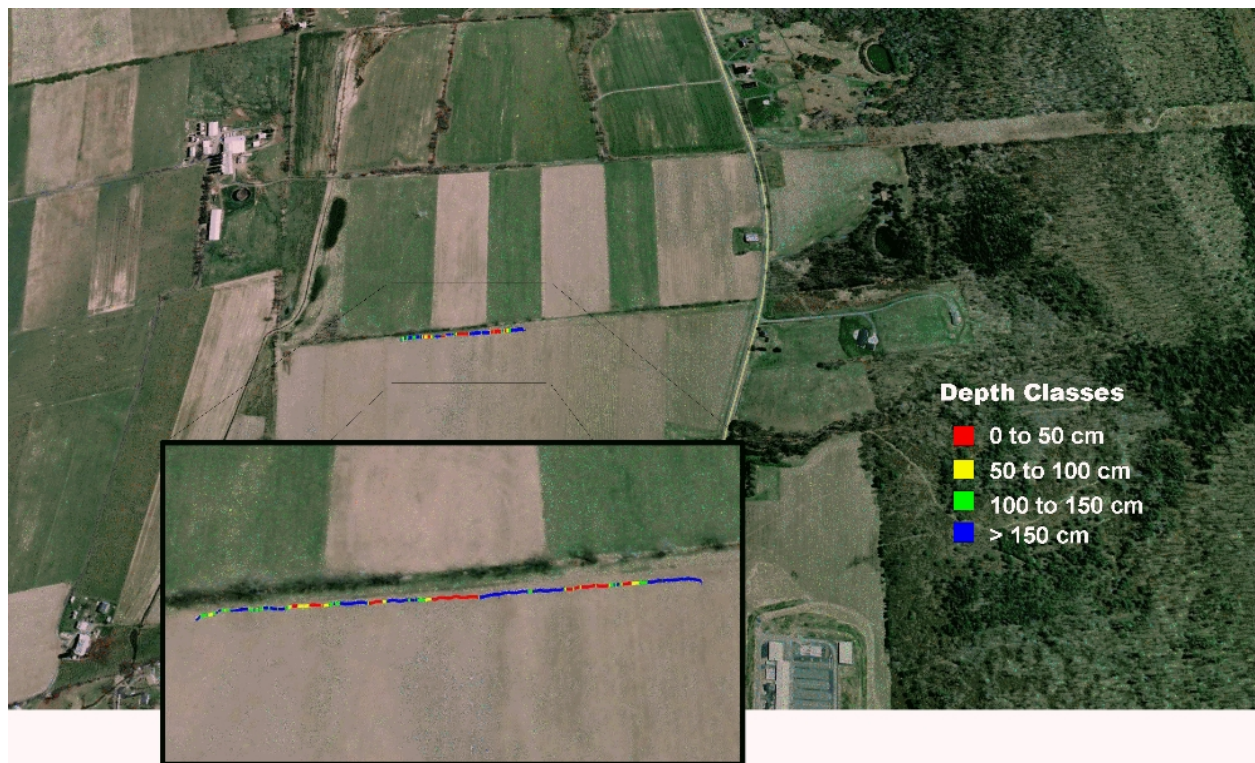


Figure 3. In this Google Earth image of the Klepler Farm site, the locations of the georeferenced GPR traverse line is shown. Colors indicate the depths to bedrock according to soil depth classes. In this area of mostly Hagerstown and Opequon soils, the depth to bedrock is predominantly very deep (> 150 cm) and shallow (<50 cm).

Using the *Interactive 3D Module* of RADAN, depths to a subsurface reflector, which was inferred to be soil-bedrock contact, were quickly picked and recorded in a layer file. This layer file was exported into an Excel worksheet for analysis. Based on 12850 measurements made on the radar record for this traverse line, the average depth to bedrock is about 128 cm, with a range of about 0 to 243 cm. Over one-half of these depth-to-bedrock measurements are between the depths of 53 and 182 cm.

Figure 3 contains Google Earth images of the area traversed with GPR at Klepler Farm. The locations and the interpreted depths to the soil-bedrock contact are shown on these images. In the area traversed with GPR, the depth to bedrock is shallow (< 50 cm) at 24 %, moderately deep (50 to 100 cm) at 10 %, deep (100 to 150 cm) at

16 %, and very deep (>150 cm) at 50 % of the measurement points (in Figure 3, these depth classes are colored red, yellow, green, and blue, respectively).

Shale Hills Area:

Three radar traverses were conducted along the northern ridge line perimeter to the Shale Hills catchment and into an adjoining catchment. Steeper portions of the traversed areas are mapped as Berks-Weikert shaly silt loams, 15 to 25 percent slopes (BiD) and Berks-Weikert association, steep (BmF). Along lower-lying and less sloping drainage channel areas, soils are mapped as Ernest silt loam, 3 to 8 percent slopes (ErB). The well drained, shallow Weikert and moderately deep Berks soils form in materials weathered from acid shales on uplands. Berks and Weikert soils are members of the loamy-skeletal, mixed, active, mesic Typic and Lithic Dystrudepts taxonomic families, respectively. The very deep, moderately well and somewhat poorly drained Ernest soils form in colluvium derived from acid shale. Ernest soils are members of the fine-loamy, mixed, superactive, mesic Aquic Fragiudults taxonomic family. All of these soils are considered to have moderately potential for GPR (<http://soils.usda.gov/survey/geography/maps/GPR/index.html>).

Using the *Interactive 3D Module* of RADAN, depths to a subsurface reflector, which was inferred to be soil-bedrock contact, were quickly picked and recorded in a layer file. This layer file was exported into an Excel worksheet for analysis. Based on 19832 interpreted measurements made along a ridgeline traverse, the average depth to bedrock is about 31 cm, with a range of about 0 to 123 cm. Over one-half of these measurements were between the depths of only about 18 and 36 cm. Along this traverse line, the depth to bedrock is shallow at 87 %, moderately deep at 12 %, and deep at 1 % of the measurement points. Figure 4 contains a Google Earth image of the area traversed with GPR near the Shale Hills Catchment (in Figure 4, different colors are used to represent the different depth classes).

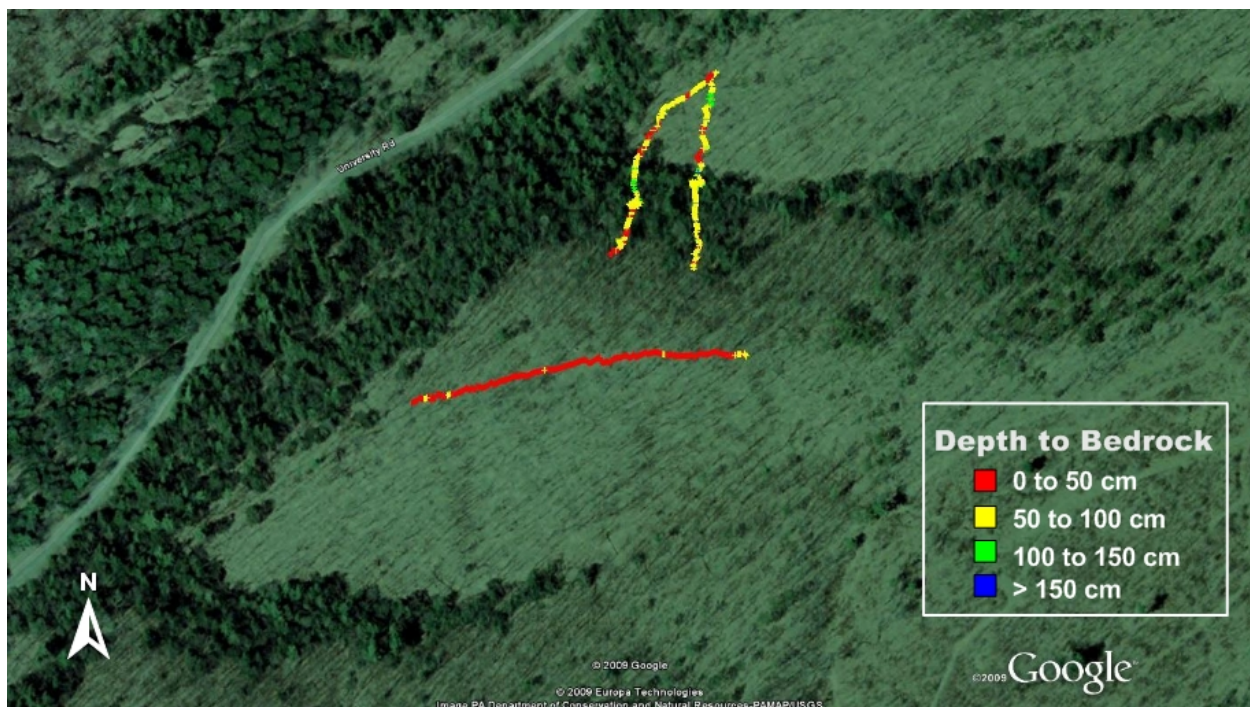


Figure 4. In this Google Earth image of the Shale Hills area site, the locations of the georeferenced GPR traverse lines are shown. Colors indicate the depths to bedrock according to soil depth classes. This contact is predominantly very deep (> 150 cm) and shallow (<50 cm) in area traversed by GPR.

Two radar traverses were conducted into the small catchment that adjoins the Shale Hills Catchment to the north. For the first traverse, based on 13707 interpreted measurements made across all three of the identified

soil map units, the average depth to bedrock is about 62 cm, with a range of about 7 to 145 cm. Over one-half of these measurements are between depths of 44 and 77 cm. Along this traverse line, the depth to bedrock is shallow at 34 %, moderately deep at 60 %, and deep at 6 % of the measurement points (in Figure 4, these depth classes are colored red, yellow, and green, respectively). For the second traverse, based on 13976 interpreted measurements made across all three of the identified soil map units, the average depth to bedrock is about 75 cm, with a range of about 12 to 159 cm. Over one-half of these measurements are between depths of 58 and 91 cm. Along this traverse line, the depth to bedrock is shallow at 17 %, moderately deep at 70 %, and deep at 13 % of the measurement points (in Figure 4, these depth classes are colored red, yellow, and green, respectively).

References:

Daniels, D. J., 2004. Ground Penetrating Radar; 2nd Edition. The Institute of Electrical Engineers, London, United Kingdom.

Jol, H., 2008. Ground Penetrating Radar: Theory and Applications. Elsevier Science, Amsterdam, The Netherlands.

Appendix 1: GPR File Numbers associated with different radar traverses and study sites.

File #	Purpose	Location
1	Buried Plate at 50 cm; 60 ns	
2	Buried Plate at 50 cm; 80 ns	
3	Buried Plate at 50 cm; 40 ns	
4 to 13	Dry Run; 60 ns	Infiltration Grid
14 to 23	Dry Run; 60 ns	Infiltration Grid
24-33	Dry Run; 80 ns	Infiltration Grid
34-43	Dry Run; 80 ns	Infiltration Grid
44-53	Dry Run; 40 ns	Infiltration Grid
54-63	11:05	Infiltration Grid
64-73	11:15	Infiltration Grid
74-83	11:25	Infiltration Grid
84-93	11:35	Infiltration Grid
94-103	11:45	Infiltration Grid
104-113	11:55	Infiltration Grid
114-123	12:05	Infiltration Grid
124-133	12:15	Infiltration Grid
DAY 2		
138-147	9:25	Infiltration Grid
148	Buried Plate at 50 cm; 60 ns	
149-160		Permanent Grid
161-172		Permanent Grid
173-182	10:25	Infiltration Grid
183-192	10:35	Infiltration Grid
193-202	10:45	Infiltration Grid
203-212	10:55	Infiltration Grid
213-222	11:05	Infiltration Grid
223-232	11:15	Infiltration Grid
233-242	11:25	Infiltration Grid
243-252	11:35	Infiltration Grid
253-262	11:45	Infiltration Grid
263-272	11:55	Infiltration Grid
277-286	15:05	Infiltration Grid